MULTI-GRID SOLUTIONS TO THE ELASTIC PLASTIC TORSION PROBLEM IN MULTIPLY CONNECTED DOMAINS

RONALD H. W. HOPPE

Technische Universität Berlin, FB Mathematik, Strasse d, 17. Juni 135, D-1000 Berlin 12, West Germany

SUMMARY

The elastic plastic torsion problem for an elastic, perfectly plastic cylinder with multiply connected cross section twisted around its longitudinal axis is formulated as an obstacle problem for an associated stress potential, the obstacle being defined in terms of a generalized distance function. Based upon the reformulation of the obstacle problem as an equivalent linear complementarity problem, the latter is discretized by means of finite difference techniques, and a monotonically convergent iterative scheme for its numerical solution is developed. At each step of the iteration the solution of a reduced system of discrete Poisson equations is required which is done by applying multi-grid techniques with respect to a hierarchy of grid-point sets. Combined with a suitably chosen nested iteration process this results in a computationally very efficient algorithm for the approximate solution of the elastic plastic torsion problem.

1. INTRODUCTION

A widely used mathematical model for the problem to determine the equilibrium of an elastic, perfectly plastic medium is the Hencky model which allows the application of the powerful apparatus of convex analysis. However, it is well known that modelling elasto-plastic phenomena by Hencky's law has its limitations, the most severe one being that the history of work hardening of the material is not taken into account. For a more detailed discussion and for a general reference to the mathematical treatment of plasticity based on Hencky's model the reader is referred to Temam's textbook.[14]

In particular, using the Hencky model, the elastic plastic torsion problem for an elastic, perfectly plastic cylinder with multiply connected cross section has been studied by Lanchon[12] and Ting[16] and numerically solved by Glowinski and Lanchon[5] and Thomasset.[15] The problem can be formulated as a constrained minimization problem for an associated energy functional or an equivalent variational inequality in terms of a related stress potential.[12] Within this mathematical setup approximate solutions can be obtained using standard relaxation-projection techniques.[5, 15] However, it is well known[6] that the convergence of these iterative methods crucially depends on a proper choice of the relaxation parameter. In other words, convergence may turn out to be rather slow if the relaxation parameter is not close to its optimal value. On the other hand, during the last decade 'optimal' iterative methods based on a recursive application of multiple grids have been developed for an efficient solution of algebraic systems arising from discretization of boundary-value problems for elliptic equations.[7, 9] In connection with variational inequalities such techniques have been successfully applied by Brandt and Cryer,[2] Hackbusch and Mittelmann[8] and by the author.[11]

In this paper, we present a computational scheme for the approximate solution of the elastic plastic torsion problem based upon its reformulation as a linear complementarity problem which is given in Section 2. In Section 3 this problem is discretized by finite difference methods and a monotonically convergent iterative procedure for its solution is presented. Section 4 shows how the computational efficiency of multi-grid techniques can be taken into account both for the solution of the algebraic systems arising at each iteration step and for the generation of an appropriate startiterate. Finally, in Section 5 several numerical results are given for various geometrical configurations of the cylinder.

2. DEFINITION OF THE PROBLEM

We consider an elastic, perfectly plastic cylindrical bar $Q:=\Omega\times[0,l]$ of cross section $\Omega\subset\mathbb{R}^2$ and length $l>0$ with m cylindrical cavities $Q_i:=\Omega_i\times[0,l]$ having the same direction of generatrices and cross section $\Omega_i\subset\Omega$, $1\leqslant i\leqslant m$, such that $\bar{\Omega}_i\cap\bar{\Omega}_j=\emptyset$, $i\neq j$, $1\leqslant i,j\leqslant m$. Denoting by $\partial Q_l:=\Omega\times\{l\}$, $\partial Q_0:=\Omega\times\{0\}$ the upper and lower ends respectively of the bar and by $\partial Q_s:=\Gamma\times(0,l)$, $\Gamma=\partial\Omega$, the lateral surface, we suppose that at ∂Q_l the bar is twisted about the x_3-axis by an angle $\theta>0$ while ∂Q_s is assumed to be stress-free.

For an isotropic material, using Hencky's law, modelling the plastic region according to the von Mises yield criterion and normalizing physical constants, it can be shown[1,2] that the equilibrium stress tensor $\{\sigma_{ij}\}$ is of the form

$$\sigma_{ij}=\begin{cases}\partial u_C/\partial x_2 & \text{for } (i,j)=(1,3) \text{ and } (i,j)=(3,1)\\ -\partial u_C/\partial x_1 & \text{for } (i,j)=(2,3) \text{ and } (i,j)=(3,2)\\ 0, & \text{otherwise } (1\leqslant i,j\leqslant 3)\end{cases}$$

The stress potential u_C is the unique solution of the constrained minimization problem

$$J_C(u_C)=\inf_{v\in K} J_C(v) \tag{1}$$

where J_C is the coercive, continuous, quadratic functional given by

$$J_C(v)=\frac{1}{2}\int_\Omega |\nabla v|^2\,\mathrm{d}x-2C\int_\Omega v\,\mathrm{d}x \tag{2}$$

C standing for the torsion angle per unit length, i.e. $C=\theta/l$, and K is the closed, convex set

$$K=\{v\in H_0^1(\Omega)\,|\,v|_{\bar{\Omega}_i}=c_i=\text{const.},\ 1\leqslant i\leqslant m,\ |\nabla v|\leqslant 1 \text{ a.e. on } \Omega\}. \tag{3}$$

Using standard arguments from convex analysis[4] it follows that $u_C\in K$ is the unique minimizer of J_C if and only if u_C satisfies the variational inequality

$$u_C\in K \tag{4a}$$

$$\int_{\Omega^*}\nabla u_C\cdot\nabla(v-u_C)\,\mathrm{d}x\geqslant 2C\int_{\Omega^*}(v-u_C)\,\mathrm{d}x,\quad v\in K \tag{4b}$$

where $\Omega^*=\Omega\backslash\{\cup_{i=1}^m\bar{\Omega}_i\}$ is the region effectively occupied by the elastic plastic material. Note that

Ω^* can be subdivided into the sets

$$\Omega^*_{E,C}=\{x\in\Omega^* \mid |\nabla u_C|<1 \text{ a.e.}\} \tag{5}$$

$$\Omega^*_{P,C}=\{x\in\Omega^* \mid |\nabla u_C|=1 \text{ a.e.}\} \tag{6}$$

characterizing the elastic and plastic region, respectively.

Setting $\Omega_0=\mathbb{R}^2\backslash\bar{\Omega}$ and $\Gamma_0=\partial\Omega_0$ we define Λ_i, $0\leqslant i\leqslant m$, as the set of directed paths from Γ_i to Γ_0, a path $P\in\Lambda_i$ consisting of directed edges $P_{i_j,i_{j+1}}$, $0\leqslant j\leqslant n-1$, $n\in\mathbb{N}$, of length $\operatorname{dist}(\Gamma_{i_j},\Gamma_{i_{j+1}})$ where $i_0=i$ and $i_n=0$. Denoting by d_i the length of the shortest path within Λ_i, we define $\psi:\Omega\to\mathbb{R}$ as the generalized distance function

$$\psi(x)=\inf_{i\in\{0,1,\ldots,m\}}\{\operatorname{dist}(x,\Omega_i)+d_i\},\quad x\in\Omega \tag{7}$$

Then, for $C\to\infty$ it can be shown[12] that the family $\{u_C\}$ of solutions to (1) converges in $H^1_0(\Omega)$ uniformly in C to $u_\infty=\psi$ with $|\nabla u_\infty|=1$ a.e. in Ω^*. Consequently, $\Omega^*_{E,\infty}=\emptyset$, $\Omega^*_{P,\infty}=\Omega^*$ and thus u_∞ represents the case of complete plastification.

The above fact motivates one to consider the modified minimization problem

$$J_C(u_C)=\inf_{v\in K'} J_C(v) \tag{8}$$

where

$$K'=\{v\in H^1_0(\Omega)\,|\,v|_{\bar{\Omega}_i}=c_i,\ 1\leqslant i\leqslant m,\ |v|\leqslant\psi \text{ a.e. on } \Omega\} \tag{9}$$

or the equivalent variational inequality

$$u_C\in K' \tag{10a}$$

$$\int_{\Omega^*}\nabla u_C\cdot\nabla(v-u_C)\,dx\geqslant 2C\int_{\Omega^*}(v-u_C)\,dx,\quad v\in K' \tag{10b}$$

Indeed, for a simply connected domain Ω, i.e. $m=0$ and thus $\psi(x)=\operatorname{dist}(x,\Omega_0)$, $x\in\Omega$, it has been shown by Brézis and Sibony[3] using a comparison principle for variational inequalities that problems (4a), (4b) and (10a), (10b) are equivalent. It is conjectured by Glowinski and Lanchon[5] that this equivalence also holds true in the multiply connected case, a conjecture which is supported by various numerical results obtained via the approximate solution of (1) and (8), respectively.

From now on we will assume $C>0$. In this case we have $u_C>0$ a.e. on Ω and hence, the constraint $|u_C|\leqslant\psi$ a.e. on Ω in the definition of K' can be replaced by $0\leqslant u_C\leqslant\psi$ a.e. on Ω. Then, taking advantage of the regularity result[12]

$$u_C\in H^1_0(\Omega)\cap C^\infty(\Omega^*)\cap C^{1,\alpha}(\bar{\Omega}^*),\quad \alpha\in(0,1) \tag{11}$$

which holds true under the assumption of piecewise smooth Γ_i, $0\leqslant i\leqslant m$, and using the fact that the lower obstacle is never active, it can be easily shown that (10a), (10b) is equivalent to the linear complementarity (LC-) problem

$$-(\Delta u_C)(x)\leqslant 2C,\quad u_C(x)\leqslant\psi(x),\quad x\in\Omega^* \tag{12a}$$

$$(\Delta u_C)(x)+2C)(u_C(x)-\psi(x))=0,\quad x\in\Omega^* \tag{12b}$$

$$u_C(x)=0,\quad x\in\Gamma,\qquad u_C(x)=c_i,\quad x\in\Gamma_i,\qquad 1\leqslant i\leqslant m \tag{12c}$$

The above LC-problem will serve as the basis for a computational scheme which will be developed in the following section.

3. THE ITERATIVE SCHEME

For the approximate solution of the LC-problem (12) we choose standard finite difference techniques with respect to a two-dimensional grid which for notational convenience will be assumed to be equidistant.

For a given step-size $h>0$ we set

$$\mathbb{R}_h^2=\{z=(z_{1,\nu_1}, z_{2,\nu_2}) \mid z_{i,\nu_i}=\nu_i h, \quad \nu_i\in\mathbb{Z}, \quad i=1,2\} \tag{13}$$

and we define

$$\Omega_h=\mathbb{R}_h^2\cap\Omega, \quad \bar{\Omega}_{h,i}=\Omega_h\cap\bar{\Omega}_i, \quad 1\leqslant i\leqslant m \tag{14a}$$

$$\Omega_h^*=\Omega_h\setminus\left(\bigcup_{i=1}^{m}\bar{\Omega}_{h,i}\right) \tag{14b}$$

Ω_h^* will be called the set of interior grid-points.

Setting $e_1=(1,0)$, $e_2=(0,1)$, $e_3=e_1+e_2$ and $e_4=e_2-e_1$, with each $z=(z_1,z_2)\in\Omega_h^*$ we associate eight neighbouring grid-points which are situated in the directions $\pm e_\nu$, $1\leqslant\nu\leqslant 4$. These directions will be referred to as east (E), west (W), north (N), south (S), north-east (NE), south-west (SW), north-west (NW) and south-east (SE), respectively, and the associated grid-points will be constructed in the following way.

Let us denote by $L_{\mathrm{SW}}(z)$ the line segment

$$L_{\mathrm{SW}}(z)=\{x=(x_1x_2)\in\mathbb{R}^2 \mid x_2=h^{-1}x_1+(z_2-h^{-1}z_1), \quad z_1-h\leqslant x_1\leqslant z_1\}$$

Then, if $L_{\mathrm{SW}}(z)\subset\Omega^*$, we set $z_{\mathrm{SW}}=(z_{\mathrm{SW},1}, z_{\mathrm{SW},2})$, $z_{\mathrm{SW},\mu}=z_\mu-h$, $1\leqslant\mu\leqslant 2$. Otherwise, we consider the non-empty set $\Gamma^*\cap L_{\mathrm{SW}}(z)$, and we define z_{SW} as the point in $\Gamma^*\cap L_{\mathrm{SW}}(z)$ which has the shortest distance to z, i.e. $\mathrm{dist}(z, z_{\mathrm{SW}})=\mathrm{dist}(z, \Gamma^*\cap L_{\mathrm{SW}}(z))$.

The line segments $L_{\mathrm{S}}(z)$, $L_{\mathrm{SE}}(z)$, ..., $L_{\mathrm{NE}}(z)$ and the corresponding neighbours z_{S}, z_{SE}, ..., z_{NE} will be constructed analogously.

We remark that for discretization with respect to a fixed grid only the four neighbouring points z_{S}, z_{W}, z_{E} and z_{N} corresponding to the standard five-point discretization of the Laplacian will be important while the neighbours z_{SW}, z_{SE}, z_{NW} and z_{NE} come into effect in the nested iteration process of a multi-grid procedure which will be described in detail in the next section.

Accordingly, we define the following sets of neighbouring grid-points

$$N_h^1(z)=\{z_{\mathrm{S}}, z_{\mathrm{W}}, z_{\mathrm{E}}, z_{\mathrm{N}}\} \tag{15a}$$

$$N_h^2(z)=N_h^1(z)\cup\{z_{\mathrm{SW}}, z_{\mathrm{SE}}, z_{\mathrm{NW}}, z_{\mathrm{NE}}\} \tag{15b}$$

and the corresponding grid-point sets

$$\Gamma_h^{*,\mu}=\left(\bigcup_{z\in\Omega_h^*}N_h^\mu(z)\right)\cap\Gamma^*, \quad 1\leqslant\mu\leqslant 2 \tag{16}$$

$$\bar{\Omega}_h^{*,\mu}=\Omega_h^*\cup\Gamma_h^{*,\mu}, \quad 1\leqslant\mu\leqslant 2 \tag{17}$$

Specifically, we set

$$\Gamma_{h,i}^{*,\mu}=\Gamma_h^{*,\mu}\cap\Gamma_i, \quad 0\leqslant i\leqslant m, \quad 1\leqslant\mu\leqslant 2 \tag{18}$$

The elements of $\Gamma_h^{*,\mu}$ and $\Gamma_{h,i}^{*,\mu}$ are called boundary grid-points while an interior grid-point $z\in\Omega_h^*$ is said to be regular if $N_h^1(z)\subset\Omega_h^*$, and irregular, otherwise.

We define $C(\Omega_h)$, $C(\Omega_h^*)$ and $C(\bar{\Omega}_h^{*,\mu})$, $1\leqslant\mu\leqslant 2$, as the vector space of real-valued grid-functions on Ω_h, Ω_h^* and $\bar{\Omega}_h^{*,\mu}$ respectively. Moreover, $C_b(\bar{\Omega}_h^{*,\mu})$, $1\leqslant\mu\leqslant 2$, refers to the subspace of $C(\bar{\Omega}_h^{*,\mu})$ given by

$$C_b(\bar{\Omega}_h^{*,\mu})=\{u_h\in C(\bar{\Omega}_h^{*,\mu})\mid u_h(z)=0,\quad z\in\Gamma_{h,0}^{*,\mu}$$
$$u_h(z)=c_i,\quad z\in\Gamma_{h,i}^{*,\mu},\quad 1\leqslant i\leqslant m\} \tag{19}$$

For a grid-function $u_h\in C(\bar{\Omega}_h^{*,1})$ and $z\in\Omega_h^*$ we define the standard forward and backward difference quotients respectively

$$(D_{h,j}^{+}u_h)(z)=(u_h(\tilde{z})-u_h(z))/(\tilde{z}_j-z_j),\quad 1\leqslant j\leqslant 2 \tag{20a}$$

$$(D_{h,j}^{-}u_h)(z)=(u_h(z)-u_h(\tilde{z}))/(z_j-\tilde{z}_j),\quad 1\leqslant j\leqslant 2 \tag{20b}$$

where $\tilde{z}=z_E$ for $j=1$, $\tilde{z}=z_N$ for $j=2$ in (20a) and $\tilde{z}=z_W$ for $j=1$, $\tilde{z}=z_S$ for $j=2$ in (20b). Further we define

$$(\delta_h^2u_h)(z)=(D_{h,1}^{+}D_{h,1}^{-}u_h)(z)+(D_{h,2}^{+}D_{h,2}^{-}u_h)(z) \tag{21}$$

as an approximation of the Laplacian.

Note that for a regular interior grid-point (21) reduces to the standard five-point discretization with respect to an equidistant grid while for an irregular interior grid-point (21) corresponds to the well-known Shortley–Weller scheme.[1]

Introducing a discrete obstacle $\psi_h\in C(\Omega_h)$ by $\psi_h=\psi|_{\Omega_h}$, we consider the discrete LC-problem

$$-(\delta_h^2u_{h,C})(z)\leqslant 2C,\quad u_{h,C}(z)\leqslant\psi_h(z),\quad z\in\Omega_h^* \tag{22a}$$

$$((\delta_h^2u_{h,C})(z)+2C)(u_{h,C}(z)-\psi_h(z))=0,\quad z\in\Omega_h^* \tag{22b}$$

$$u_{h,C}(z)=0,\quad z\in\Gamma_{h,0}^{*,1},\quad u_{h,C}(z)=c_i,\quad z\in\Gamma_{h,i}^{*,1},\quad 1\leqslant i\leqslant m \tag{22c}$$

We can formally rewrite (22) as the Hamilton–Jacobi–Bellman (HJB-) equation

$$\max[(-\delta_h^2u_{h,C})(z)-2C,\quad u_{h,C}(z)-\psi_h(z)]=0,\quad z\in\Omega_h^* \tag{23a}$$

$$u_{h,C}(z)=0,\quad z\in\Gamma_{h,0}^{*,1},\quad u_{h,C}(z)=c_i,\quad z\in\Gamma_{h,i}^{*,1},\quad 1\leqslant i\leqslant m \tag{23b}$$

Assuming that for increasing C the plastification spreads from Γ_i, $0\leqslant i\leqslant m$, it is natural to take $c_i=d_i$, $1\leqslant i\leqslant m$. Then, setting $N_h=\operatorname{card}\Omega_h^*$, (23) is a system of N_h non-linear difference equations in the N_h unknowns $u_h(z)$, $z\in\Omega_h^*$. Following the arguments used for discrete LC-problems and discrete HJB-equations[10] it can be easily shown that (22) or (23) admit a unique solution $u_{h,C}\in C_b(\bar{\Omega}_h^{*,1})$ which approximates the solution u_C to (12) of order $O(h^\alpha)$ provided $u_C\in C^{2,\alpha}(\bar{\Omega}^*)$, $\alpha\in(0,1)$. Moreover, in view of the regularity result (11) interior estimates of order $O(h^2)$ can be expected.

We now present a monotonic convergent iterative scheme for the solution of the discrete LC-problem (22) which has been successfully used for discrete HJB-equations.[10,13] At each iteration step this scheme requires the solution of a reduced linear algebraic system which can be constructed in the following way.

Given an iterate $u_{h,C}^{\nu}\in C_b(\bar{\Omega}_h^{*,1})$, $\nu\geqslant 0$, we set $d_{h,C}^{1,(\nu)}=(-\delta_h^2u_{h,C}^{\nu})(z)-2C$, $d_{h,C}^{2,(\nu)}(z)=u_{h,C}^{\nu}(z)-\psi_h(z)$, $z\in\Omega_h^*$, and we define a difference operator $A_h^{(\nu)}:C_b(\bar{\Omega}_h^{*,1})\to C(\Omega_h^*)$ and a grid-function $f_h^{(\nu)}\in C(\Omega_h^*)$

by

$$(A_h^{(\nu)}v_h)(z)=\begin{cases}(-\delta_h^2 v_h)(z), & \text{if } d_{h,C}^{1,(\nu)}(z)>d_{h,C}^{2,(\nu)}(z)\\ v_h(z), & \text{otherwise}\end{cases} \tag{24}$$

$$f_h^{(\nu)}(z)=\begin{cases}2C, & \text{if } d_{h,C}^{1,(\nu)}(z)>d_{h,C}^{2,(\nu)}(z)\\ \psi_h(z), & \text{otherwise}\end{cases} \tag{25}$$

Then, a new iterate $u_{h,C}^{\nu+1}\in C_b(\bar{\Omega}_h^{*,1})$ will be computed as the solution of

$$(A_h^{(\nu)}u_{h,C}^{\nu+1})(z)=f_h^{(\nu)}(z), \quad z\in\Omega_h^* \tag{26}$$

The definitions of $A_h^{(\nu)}$ and $f_h^{(\nu)}$ induce a partition of Ω_h^* according to

$$\Omega_h^*=\Omega_h^{*,(1)}(u_{h,C}^{\nu})\cup\Omega_h^{*,(2)}(u_{h,C}^{\nu}),\ \Omega_h^{*,(1)}(u_{h,C}^{\nu})\cap\Omega_h^{*,(2)}(u_{h,C}^{\nu})=\emptyset \tag{27}$$

where

$$\Omega_h^{*,(1)}(u_h^{\nu})=\{z\in\Omega_h^*\mid d_{h,C}^{1,(\nu)}(z)>d_{h,C}^{2,(\nu)}(z)\} \tag{28a}$$

$$\Omega_h^{*,(2)}(u_h^{\nu})=\{z\in\Omega_h^*\mid d_{h,C}^{1,(\nu)}(z)\leqslant d_{h,C}^{2,(\nu)}(z)\} \tag{28b}$$

Setting $N_h^{\mu}=\operatorname{card}\Omega_h^{*,(\mu)}(u_{h,C}^{\nu})$, $1\leqslant\mu\leqslant 2$, we have $u_{h,C}^{\nu+1}=\psi_h(z)$, $z\in\Omega_h^{*,(2)}(u_{h,C}^{\nu})$, and hence (26) reduces to a system of N_h^1 linear equations in the N_h^1 unknowns $u_{h,C}^{\nu+1}(z)$, $z\in\Omega_h^{*,(1)}(u_{h,C}^{\nu})$.

Since $\Omega_h^{*,(2)}(u_{h,C}^{\nu})$ represents the set of grid-points where the discrete obstacle function ψ_h is active, grid-points $z\in\Omega_h^{*,(2)}(u_{h,C}^{\nu})$ are said to be active while grid-points $z\in\Omega_h^{*,(1)}(u_{h,C}^{\nu})$ are called inactive. For the exact solution $u_{h,C}$ to (22) or (23) the set $\Omega_h^{*,(2)}(u_{h,C})$ characterizes the discrete coincidence set which indicates the discrete region of plastification.

Denoting by $\|\cdot\|_{h,\infty}$ the maximum norm in $C(\Omega_h^*)$ and prespecifying an accuracy bound $\varepsilon_h^1>0$ as termination criterion for the iteration, the complete algorithm EPT$(u_{h,C},\varepsilon_h^1,C)$ for the solution of the elastic plastic torsion problem with the torsion angle per unit length C and the accuracy bound ε_h^1 as inputs and an approximate solution $u_{h,C}$ as output reads as follows.

ALGORITHM EPT$(u_{h,C},\varepsilon_h^1,C)$:

Step 1. Choose a start-iterate $u_h^0\in C_b(\bar{\Omega}_h^{*,1})$ and set $\nu=0$.

Step 2. Determine $A_h^{(\nu)}$ and $f_h^{(\nu)}$ according to (24), (25) and compute $u_{h,C}^{\nu+1}\in C_b(\bar{\Omega}_h^{*,1})$ as the solution to (26).

Step 3. If $\|u_{h,C}^{\nu+1}-u_{h,C}^{\nu}\|_{h,\infty}<\varepsilon_h^1$, then set $u_{h,C}=u_{h,C}^{\nu+1}$ and stop the algorithm, otherwise set $\nu=\nu+1$ and go to Step 2.

Recalling that a grid-function $w_h\in C_b(\bar{\Omega}_h^{*,1})$ is said to be a supersolution to (23) if

$$\max[(-\delta_h^2 w_h)(z)-2C,\ w_h(z)-\psi_h(z)]\geqslant 0, \quad z\in\Omega_h^* \tag{29}$$

we have the following convergence result.[11]

Theorem

For given $C>0$ let $u_h^0\in C_b(\bar{\Omega}_h^{*,1})$ be a supersolution to (23). Then, the sequence $\{u_{h,C}^{\nu}\}_{\nu\geqslant 0}$ of iterates $u_{h,C}^{\nu}\in C_b(\bar{\Omega}_h^{*,1})$ governed by the algorithm EPT$(u_{h,C},0,C)$ is a monotonically decreasing sequence of grid-functions converging for $\nu\to\infty$ to the unique solution $u_{h,C}$ of (23).

Proof. For $\nu\geqslant 1$ we have

$$\begin{aligned}&\max[(-\delta_h^2 u_{h,C}^{\nu})(z)-2C,\ u_{h,C}^{\nu}(z)-\psi_h(z)]\\ &\geqslant(A_h^{(\nu-1)}u_{h,C}^{\nu})(z)-f_h^{(\nu-1)}(z)=0, \quad z\in\Omega_h^*\end{aligned} \tag{30}$$

and hence, each iterate $u_{h,C}^{\nu}$, $\nu \geqslant 0$, is a supersolution to (23). Consequently,

$$(A_h^{(\nu-1)} u_h^{(\nu-1)})(z) - f_h^{(\nu-1)}(z) \geqslant 0, \quad z \in \Omega_h^* \tag{31}$$

Moreover,

$$\begin{aligned} 0 &= \max[(-\delta_h^2 u_{h,C})(z) - 2C, u_{h,C}(z) - \psi_h(z)] \\ &\geqslant (A_h^{(\nu-1)} u_{h,C})(z) - f_h^{(\nu-1)}(z), \quad z \in \Omega_h^* \end{aligned} \tag{32}$$

Since for each $\nu \geqslant 1$ the operator $A_h^{(\nu-1)}$ satisfies the maximum principle

$$A_h^{(\nu-1)} v_h \geqslant A_h^{(\nu-1)} w_h \Rightarrow v_h \geqslant w_h, \quad v_h, w_h \in C_b(\bar{\Omega}_h^{*,1})$$

inequalities (30), (31) and (32) yield $u_{h,C}^{\nu-1} \geqslant u_{h,C}^{\nu} \geqslant u_{h,C}$, $\nu \geqslant 1$. This implies the existence of a grid-function $u_{h,C}^* \in C_b(\bar{\Omega}_h^{*,1})$ such that $u_{h,C}^{\nu}(z) \to u_{h,C}^*(z)$, $z \in \Omega_h^*$, for $\nu \to \infty$. In view of

$$\begin{aligned} &\max[(-\delta_h^2 u_{h,C}^{\nu-1})(z) - 2C, u_{h,C}^{\nu-1}(z) - \psi_h(z)] \\ &= (A_h^{(\nu-1)} u_{h,C}^{\nu-1})(z) - f_h^{(\nu-1)}(z) = (A_h^{(\nu-1)}(u_{h,C}^{\nu-1} - u_{h,C}^{\nu}))(z) \end{aligned}$$

for $\nu \to \infty$ we get

$$\max[(-\delta_h^2 u_{h,C}^*)(z) - 2C, u_{h,C}^*(z) - \psi_h(z)] = 0, \quad z \in \Omega_h^*$$

whence $u_{h,C}^* = u_{h,C}$ because of the unique solvability of (23).

Bearing in mind that the solution $u_{h,C}$ to (23) satisfies the strict complementary slackness condition

$$(-\delta_h^2 u_{h,C})(z) < 2C, \quad z \in \Omega_h^{*,(2)}(u_{h,C}) \tag{33}$$

it can be shown that convergence occurs after a finite number of steps. In particular, we have the following.

Corollary

Under the assumptions of the preceding theorem there exist indices $\nu_0, \nu_1 \in \mathbb{N}$, $\nu_1 \geqslant \nu_0$, such that

$$\Omega_h^{*,(2)}(u_{h,C}) \subseteq \Omega_h^{*,(2)})(u_{h,C}^{\nu+1}) \subseteq \Omega_h^{*,(2)}(u_{h,C}^{\nu}), \quad \nu \geqslant \nu_0 \tag{34}$$

and

$$\Omega_h^{*,(2)}(u_{h,C}^{\nu}) = \Omega_h^{*,(2)}(u_{h,C}), \quad u_{h,C}^{\nu} = u_{h,C}, \quad \nu \geqslant \nu_1 \tag{35}$$

Proof. The proof is by contradiction arguments. If the first inclusion in (34) does not hold, there exist a subsequence $\mathbb{N}' \subset \mathbb{N}$ and a grid-point $z \in \Omega_h^*$ with $z \in \Omega_h^{*,(2)}(u_{h,C})$ but $z \notin \Omega_h^{*,(2)}(u_{h,C}^{\nu})$, $\nu \in \mathbb{N}'$. Consequently, $(-\delta_h^2 u_{h,C})(z) - 2C < 0$ and $(-\delta_h^2 u_{h,C}^{\nu+1})(z) - 2C = 0$, $\nu \in \mathbb{N}'$, contradicting the fact that $(-\delta_h^2 u_{h,C}^{\nu+1})(z) - 2C \to (-\delta_h^2 u_{h,C})(z) - 2C$ for $\nu \to \infty$, $\nu \in \mathbb{N}'$.

Similarly, if the second inclusion is not true, there exist another subsequence $\mathbb{N}'' \subset \mathbb{N}$ and a grid-point $z \in \Omega_h^*$ such that $z \in \Omega_h^{*,(2)}(u_{h,C}^{\nu+1})$ but $z \notin \Omega_h^{*,(2)}(u_{h,C}^{\nu})$, $\nu \in \mathbb{N}''$, whence

$$(-\delta_h^2 u_{h,C}^{\nu})(z) - 2C > u_{h,C}^{\nu}(z) - \psi_h(z) \geqslant u_{h,C}^{\nu+1}(z) - \psi_h(z) \geqslant (-\delta_h^2 u_{h,C}^{\nu+1})(z) - 2C = 0$$

For $\nu \to \infty$ this gives $u_{h,C}(z) - \psi_h(z) = 0$ and $(-\delta_h^2 u_{h,C})(z) - 2C = 0$, contradicting the strict complementary slackness condition (33).

Finally, since there is only a finite number of constraints, there must be an integer $\nu_1 \geqslant \nu_0$ such that (34) holds true and thus $u_{h,C}^{\nu_1} = u_{h,C}$.

The assumption on the start-iterate $u_{h,C}^0 \in C_b(\bar{\Omega}_h^{*,1})$ to be a supersolution to (23) can be dispensed with. Indeed, if $u_{h,C}^0 \in C_b(\bar{\Omega}_h^{*,1})$ is chosen arbitrarily, then it is guaranteed that after one iteration we end up with a supersolution $u_{h,C}^1$, and thus we obtain monotonic convergence of the sequence $\{u_{h,C}^\nu\}_{\nu \geq 1}$. When using multiple grids this global convergence property is of importance in the so-called nested iteration process, as will be described in the next section.

4. THE MULTI-GRID ALGORITHMS

As has been shown in the last section, the implementation of the iterative procedure EPT($u_{h,C}$, ε_h^1, C) requires the successive solution of discrete Poisson equations with respect to an increasing sequence of grid-point sets $\Omega_h^{*,(1)}(u_{h,C}^\nu)$, $\nu \in \mathbb{N}$. Since in view of the geometry of these sets fast-Poisson solvers are not applicable, and since standard iterative solvers like Gauss–Seidel overrelaxation suffer from poor convergence, we recommend the application of multi-grid techniques with respect to a hierarchy $\{\mathbb{R}_k^2\}_{k=0}^l$ of equidistant grids with step-sizes $h_{k+1} < h_k$, $0 \leq k \leq l-1$. For simplicity we assume $h_{k+1} = h_k/2$, $0 \leq k \leq l-1$, given some $h_0 > 0$.

By Ω_k, $\bar{\Omega}_{k,i}$ $(1 \leq i \leq m)$, Ω_k^* and $\bar{\Omega}_k^{*,\mu}$ $(1 \leq \mu \leq 2)$, $0 \leq k \leq 1$, we denote the grids defined according to (14), (17) while δ_k^2, $0 \leq k \leq l$, refers to the discrete Laplacian on $C_b(\bar{\Omega}_h^{*,1})$ constructed by means of (21). Then, in contrast to standard multi-grid methods for discrete Poisson equations,[7,9] the problem which arises in connection with equation (26) on the finest grid $\bar{\Omega}_l^{*,1}$ is how to specify the sets $\Omega_k^{*,(\mu)}(u_{l,C}^\nu)$, $1 \leq \mu \leq 2$, $\nu \geq 0$, of active/inactive grid-points on the lower levels $0 \leq k < l$. In order to avoid that discrete free boundaries remain undetected it is recommended[8,11] to specify an interior grid-point $z \in \Omega_h^*$, $k < l$, as inactive, if z and all its eight neighbours from $N_{k+1}^2(z)$ are inactive on level $k+1$. This means, given $\Omega_l^{*,(1)}(u_{l,C}^\nu)$, we define $\Omega_k^{*,(1)}(u_{l,C}^\nu)$, $0 \leq k < l$, recursively by

$$\Omega_k^{*,(1)}(u_{l,C}^\nu) = \{z \in \Omega_{k+1}^{*,(1)}(u_{l,C}^\nu) \mid N_{k+1}^2(z) \subset \Omega_{k+1}^{*,(1)}(u_{l,C}^\nu)\} \tag{36}$$

We set $\Omega_k^{*,(2)}(u_{l,C}^\nu) = \Omega_k^* \setminus \Omega_k^{*,(1)}(u_{l,C}^\nu)$, $0 \leq k \leq l$, and we define $k_{\min}$ as the smallest integer $0 \leq k \leq l$ for which $\Omega_k^{*,(1)}(u_{l,C}^\nu) \neq \emptyset$, i.e. $\Omega_{k_{\min}}^*$ is the coarsest grid with at least one inactive grid-point.

For the coarse-to-fine and the fine-to-coarse transfers within a multi-grid cycle we have to provide suitable prolongations and restrictions. We denote by $p_k^{k+1}: \mathbb{R}_k^2 \to \mathbb{R}_{k+1}^2$, $0 \leq k \leq l-1$, the prolongation based upon bilinear interpolation and by $r_{k+1}^k: \mathbb{R}_{k+1}^2 \to \mathbb{R}_k^2$, $0 \leq k \leq l-1$, the corresponding full weighted restriction.[7,9] Further, if $v_k \in C(\Omega_k^*)$ or $v_k \in C_b(\Omega_k^{*,1})$, $0 \leq k < l$, we introduce a grid-function $\tilde{v}_k \in C(\mathbb{R}_k^2)$ by

$$\tilde{v}_k(z) = \begin{cases} v_k(z), & \text{if } z \in \Omega_k^{*,(1)}(u_{l,C}^\nu) \\ 0, & \text{otherwise} \end{cases}$$

Then, we define prolongations $\tilde{p}_k^{k+1}: C_b(\bar{\Omega}_k^{*,1}) \to C(\Omega_{k+1}^*)$ and restrictions $\tilde{r}_{k+1}^k: C(\Omega_{k+1}^*) \to C(\Omega_k^*)$ or $\tilde{r}_{k+1}^k: C_b(\bar{\Omega}_{k+1}^{*,1}) \to C(\Omega_{k+1}^*)$, $0 \leq k \leq l-1$, according to

$$(\tilde{p}_k^{k+1} v_k)(z) = \begin{cases} (p_k^{k+1} \tilde{v}_k)(z), & \text{if } z \in \Omega_{k+1}^{*,(1)}(u_{l,C}^\nu) \\ 0, & \text{otherwise} \end{cases} \tag{37}$$

$$(\tilde{r}_{k+1}^k v_{k+1})(z) = \begin{cases} (r_{k+1}^k \tilde{v}_{k+1})(z), & \text{if } z \in \Omega_k^{*,(1)}(u_{l,C}^\nu) \\ 0, & \text{otherwise} \end{cases} \tag{38}$$

Further, we need a suitable smoothing procedure for the reduced linear system (26) on level $k = l$ and for the defect correction equations on levels $k_{\min} < k < l$ as well as a solver for the defect correction equation on the coarsest grid. For both purposes we propose Gauss–Seidel iteration, denoting the application of κ Gauss–Seidel iterations to the corresponding equation on level k by

$$w_k = S_k(v_k; \kappa) \tag{39}$$

where $v_k \in C_b(\bar{\Omega}_k^{*,1})$ is used as a start-iterate. Note that the defect correction equations on levels $k_{\min} \leqslant k < l$ are given by

$$(A_k^{(\nu)} u_{k,C}^{\nu+1})(z) - f_k^{(\nu)}(z) = 0, \quad z \in \Omega_k^* \tag{40}$$

where the operator $A_k^{(\nu)}: C_b(\bar{\Omega}_k^{*,1}) \to C(\Omega_k^*)$ and the grid-function $f_k^{(\nu)} \in C(\Omega_k^*)$ are defined according to

$$(A_k^{(\nu)} v_k)(z) = \begin{cases} (-\delta_k^2 v_k)(z), & \text{if } z \in \Omega_k^{*,(1)}(u_{l,C}^{\nu}) \\ v_k(z), & \text{if } z \in \Omega_k^{*,(2)}(u_{l,C}^{\nu}) \end{cases} \tag{41}$$

$$f_k^{(\nu)}(z) = (A_k^{(\nu)} v_{k,C}^{\nu})(z) - (\tilde{r}_{k+1}^k (A_{k+1}^{(\nu)} \bar{u}_{k+1,C}^{\nu} - f_{k+1}^{(\nu)}))(z) \tag{42}$$

$\bar{u}_{k+1,C}^{\nu}$ denoting the smoothed iterate on level $k+1$ and $v_{k,C}^{\nu} \in C_b(\bar{\Omega}_k^{*,1})$ given by

$$v_{k,C}^{\nu}(z) = \begin{cases} (\tilde{r}_{k+1}^k \bar{u}_{k+1,C}^{\nu})(z), & \text{if } z \in \Omega_k^{*,(1)}(u_{l,C}^{\nu}) \\ \psi_k(z), & \text{if } z \in \Omega_k^{*,(2)}(u_{l,C}^{\nu}) \\ d_i, & \text{if } z \in \Gamma_{k,i}^{*,1} (1 \leqslant i \leqslant m) \\ 0, & \text{if } z \in \Gamma_{k,0}^{*,1} \end{cases} \tag{43}$$

If $k = l$, we set $v_{l,C}^{\nu} = u_{l,C}^{\nu}$.

The following algorithm $\mathrm{MG}(u_{k,C}^{\nu+1}, v_{k,C}^{\nu}, k)$ describes a complete multi-grid cycle for computation of an approximation $u_{k,C}^{\nu+1} \in C_b(\bar{\Omega}_k^{*,1})$ to (26), if $k = l$, or to (40), if $k < l$, given $v_{k,C}^{\nu} \in C_b(\bar{\Omega}_k^{*,1})$ as a start-iterate.

ALGORITHM $\mathrm{MG}(u_{k,C}^{\nu+1}, v_{k,C}^{\nu}, k)$:

Step 1. If $k = k_{\min}$, compute $u_{k,C}^{\nu+1}$ by κ_3 Gauss–Seidel iterations applied to (40) on level $k_{\min}$, i.e.

$$u_{k,C}^{\nu+1} = S_k(v_{k,C}^{\nu}; \kappa_3) \tag{44}$$

Step 2. If $k > k_{\min}$, compute a smoothed iterate $\bar{u}_{k,C}^{\nu}$ by κ_1 Gauss–Seidel iterations applied to (26), if $k = l$, or to (40), if $k < l$, i.e.

$$\bar{u}_{k,C}^{\nu} = S_k(v_{k,C}^{\nu}; \kappa_1) \tag{45}$$

Step 3. Determine the operator $A_{k-1}^{(\nu)}$ and the grid-functions $f_{k-1}^{(\nu)}$, $v_{k-1,C}^{\nu}$ by means of (41), (42), (43) and compute $u_{k-1,C}^{\nu+1}$ by applying γ_{k-1} cycles $\mathrm{MG}(u_{k-1,C}^{\nu+1}, v_{k-1,C}^{\nu}, k-1)$.

Step 4. Compute $\bar{\bar{u}}_{k,C}^{\nu} \in C_b(\bar{\Omega}_k^{*,1})$ by

$$\bar{\bar{u}}_{k,C}^{\nu} = \bar{u}_{k,C}^{\nu} - \tilde{p}_{k-1}^k [\tilde{r}_k^{k-1} \bar{u}_{k,C}^{\nu} - u_{k-1,C}^{\nu+1}] \tag{46}$$

and determine $u_{k,C}^{\nu+1}$ by κ_2 Gauss–Seidel iterations applied to (26), if $k = l$, or to (40), if $k < l$, using $\bar{\bar{u}}_{k,C}^{\nu}$ as start-iterate, i.e.

$$u_{k,C}^{\nu+1} = S_k(\bar{\bar{u}}_{k,C}^{\nu}; \kappa_2) \tag{47}$$

Finally, if $k < l$, set $v_{k,C}^{\nu} = u_{k,C}^{\nu+1}$.

Due to the definition of $\tilde{p}_k^{k+1}$ and $\tilde{r}_{k+1}^k$ (cf. (37), (38)) and the fact that the smoothing procedure only changes values in $z \in \Omega_k^{*,(1)}(u_{l,C}^{\nu})$, it follows from (45), (46) and (47) that the prespecified values $\psi_k(z)$ in $z \in \Omega_k^{*,(2)}(u_{l,C}^{\nu})$ remain unchanged while performing a multi-grid cycle.

Choosing an accuracy bound $\varepsilon_l^2 > 0$ as termination criterion for the multi-grid iterations, the iterative procedure EPT of Section 3 can be coupled with the multi-grid scheme MG to give an effective algorithm $\mathrm{MGEPT}(u_{l,C}, \varepsilon_l^1, \varepsilon_l^2, C)$ for computing an approximation $u_{l,C} \in C_b(\bar{\Omega}_l^{*,1})$ to the LC-problem (12) on level l. This algorithm results if in $\mathrm{EPT}(u_{h,C}, \varepsilon_h^1, C)$ we take $h = h_l$ and replace Step 2 by

Step 2'. (i) Determine $A_l^{(\nu)}, f_l^{(\nu)}$ and the sets $\Omega_k^{*,(\eta)}(u_{l,C}^{\nu})$, $1 \leqslant \eta \leqslant 2$, $k_{\min} \leqslant k \leqslant l$, according to (24), (25), (28), (36), set $u_{l,C}^{\nu+1,0} = v_{l,C}^{\nu} = u_{l,C}^{\nu}$ and $\mu = 0$.

(ii) Set $\mu = \mu + 1$ and determine $u_{l,C}^{\nu+1,\mu}$ by performing MG($u_{l,C}^{\nu+1,\mu}$, $v_{l,C}^{\nu}$, l).

(iii) If $\|u_{l,C}^{\nu+1,\mu} - u_{l,C}^{\nu+1,\mu-1}\|_{l,\infty} < \varepsilon_l^2$, set $u_{l,C}^{\nu+1} = u_{l,C}^{\nu+1,\mu}$ and go to Step 3, otherwise set $v_{l,C}^{\nu} = u_{l,C}^{\nu+1,\mu}$ and go to Step 2'(ii).

The performance of the multi-grid algorithm MGEPT can be considerably improved by choosing an appropriate start-iterate $u_{l,C}^0$ on the finest grid. This can be achieved by nested iteration.[7,9]

Starting from a grid-function $u_{0,C}^0$ on the coarsest grid, at each level $0 \leqslant k < l$ an approximation $u_{k,C}$ is computed by perfoming a multi-grid cycle involving the grids $0 \leqslant m \leqslant k$, and $u_{k,C}$ is then interpolated to the level $k+1$ by a suitable prolongation process. For this purpose we cannot use the prolongation operator $\tilde{p}_k^{k+1}$ as defined by (37), since $\tilde{p}_k^{k+1}$ is specially designed for the coarse-to-fine transfer within MG already assuming the knowledge of an approximation on level $k+1$. Therefore, we construct another prolongation operator $\hat{p}_k^{k+1}: C_b(\bar{\Omega}_k^{*,1}) \to C(\Omega_{k+1}^*)$ in the following way.

If $v_k \in C_b(\bar{\Omega}_k^{*,1})$ and $z \in \Omega_{k+1}^* \setminus \Omega_k^*$, we define $\hat{v}_k(z')$, $z' \in N_{k+1}^2(z)$, by

$$\hat{v}_k(z') = \begin{cases} v_k(z'), & \text{if } z' \in \Omega_k^* \\ 0, & \text{if } z' \in \Gamma_{k+1,0}^{*,2} \\ d_i, & \text{if } z' \in \Gamma_{k+1,i}^{*,2}, \quad 1 \leqslant i \leqslant m \end{cases}$$

where (i) $z' = z_W, z_E$, if $z \pm h_{k+1} e_1 \in \mathbb{R}_k^2$, (ii) $z' = z_S, z_N$, if $z \pm h_{k+1} e_2 \in \mathbb{R}_k^2$ and (iii) $z' = z_{SW}, z_{SE}, z_{NW}, z_{NE}$, if $z \pm h_{k+1} e_\mu \in \mathbb{R}_k^2$, $\mu = 3, 4$.

We then define $(\hat{p}_k^{k+1} v_k)(z)$ by $(\hat{p}_k^{k+1} v_k)(z) = v_k(z)$, if $z \in \Omega_k^*$, and, if $z \notin \Omega_k^*$, by linear interpolation between $\hat{v}_k(z_W)$ and $\hat{v}_k(z_E)$ in case (i) or $\hat{v}_k(z_S)$, $\hat{v}_k(z_N)$ in case (ii), and by bilinear interpolation between $\hat{v}_k(z_{SW})$, $\hat{v}_k(z_{SE})$, $\hat{v}_k(z_{NW})$, $\hat{v}_k(z_{NE})$ in case (iii).

Now, if $u_{k,C} \in C_b(\bar{\Omega}_k^{*,1})$, we define $u_{k+1,C}^0 \in C_b(\bar{\Omega}_{k+1}^{*,1})$ by first specifying the sets $\Omega_{k+1}^{*,(\mu)}(u_{k+1,C}^0)$, $1 \leqslant \mu \leqslant 2$, according to

$$\Omega_{k+1}^{*,(2)}(u_{k+1,C}^0) = \{z \in \Omega_{k+1}^* \mid N_{k+1}^2(z) \cap \Omega_k^* \subset \Omega_k^{*,(2)}(u_{k,C})\},$$
$$\Omega_{k+1}^{*,(1)}(u_{k+1,C}^0) = \Omega_{k+1}^* \setminus \Omega_{k+1}^{*,(2)}(u_{k+1,C}^0)$$

and then setting

$$u_{k+1,C}^0(z) = \begin{cases} (\hat{p}_k^{k+1} u_{k,C})(z), & \text{if } z \in \Omega_{k+1}^{*,(1)}(u_{k+1,C}^0) \\ \psi_{k+1}(z), & \text{if } z \in \Omega_{k+1}^{*,(2)}(u_{k+1,C}^0) \\ 0, & \text{if } z \in \Gamma_{k+1,0}^{*,1} \\ d_i, & \text{if } z \in \Gamma_{k+1,i}^{*,1}, \quad 1 \leqslant i \leqslant m. \end{cases} \tag{48}$$

Prespecifying accuracy bounds $\varepsilon_k^\mu > 0$, $\mu = 1, 2$, on all levels $0 \leqslant k \leqslant l$, the nested iteration process combined with the scheme MGEPT results in

ALGORITHM NMGEPT($u_{l,C}$, $(\varepsilon_k^1)_{k=0}^l$, $(\varepsilon_k^2)_{k=0}^l$, C):

Step 1. Set $k = 0$, choose $u_{0,C}^0 \in C_b(\bar{\Omega}_0^{*,1})$ by $u_{0,C}^0(z) = \psi_0(z)$, $z \in \Omega_0^*$, and compute $u_{0,C}$ by performing MGEPT($u_{0,C}$, ε_0^1, ε_0^2, C).

Step 2. Set $k = k+1$, determine $u_{k,C}^0$ by (48) and compute $u_{h,C}$ by performing MGEPT($u_{k,C}$, ε_k^1, ε_k^2, C).

Step 3. If $k = l$, stop the algorithm, otherwise go to Step 2.

We remark that in general the interpolated startiterate $u_{k,C}^0$ is not a supersolution to (23) on level k, but due to the global convergence of the scheme EPT this does not affect the convergence of the nested iteration scheme.

5. NUMERICAL RESULTS

As test examples we have chosen cylinders with a different number m of cavities having circular or rectangular cross sections Ω and Ω_i respectively, $1 \leqslant i \leqslant m$, and being subjected to a torsion of varying twist angle per unit length C.

In particular, we have considered the following cases,

I. Circular cross sections

$$\Omega = \{(x_1, x_2) \mid (x_1 - 0{\cdot}5)^2 + (x_2 - 0{\cdot}5)^2 < 0{\cdot}25\}$$

$$\Omega_i = \{(x_1, x_2) \mid (x_1 - x_1^i)^2 + (x_2 - x_2^i)^2 < r_i^2\}, \quad 1 \leqslant i \leqslant m$$

(i) $m = 0$ [cf. Figures 1, 5]

(ii) $m = 2$ [cf. Figures 3, 8]

$x_1^1 = x_2^1 = x_2^2 = 0{\cdot}5,\ x_1^2 = 0{\cdot}825,\ r_1 = r_2 = 0{\cdot}125$

(iii) $m = 9$ [cf. Figures 4, 11]

$x_1^1 = 0{\cdot}5,\ x_2^1 = 0{\cdot}5,\ r_1 = 0{\cdot}2$

$x_1^2 = 0{\cdot}15,\ x_2^2 = 0{\cdot}5;\ x_1^3 = x_2^3 = 0{\cdot}25$

$x_1^4 = 0{\cdot}25,\ x_2^4 = 0{\cdot}75;\ x_1^5 = 0{\cdot}5,\ x_2^5 = 0{\cdot}15$

$x_1^6 = 0{\cdot}5,\ x_2^6 = 0{\cdot}85;\ x_1^7 = 0{\cdot}75,\ x_2^7 = 0{\cdot}25$

$x_1^8 = x_2^8 = 0{\cdot}75;\ x_1^9 = 0{\cdot}85,\ x_2^9 = 0{\cdot}5$

$r_i = 0{\cdot}05,\ 2 \leqslant i \leqslant 9$

II. Rectangular cross sections

$$\Omega = \{(x_1, x_2) \mid 0 < x_1 < 1,\ 0 < x_2 < 1\},$$

$$\Omega_i = \{(x_1, x_2) \mid a_1^i < x_1 < b_1^i,\ a_2^i < x_2 < b_2^i\}, \quad 1 \leqslant i \leqslant m$$

(i) $m = 0$ [cf. Figures 2, 6]

(ii) $m = 1$ [cf. Figure 7]

$a_1^1 = 0{\cdot}2,\ b_1^1 = 0{\cdot}5,\ a_2^1 = 0{\cdot}65,\ b_2^1 = 0{\cdot}95$

(iii) $m = 2$ [cf. Figure 9]

$a_1^1 = 0{\cdot}2,\ b_1^1 = 0{\cdot}4,\ a_2^1 = 0{\cdot}2,\ b_2^1 = 0{\cdot}8$

$a_1^2 = 0{\cdot}6,\ b_1^2 = 0{\cdot}8,\ a_2^2 = 0{\cdot}2,\ b_2^2 = 0{\cdot}8$

(iv) $m = 4$ [cf. Figure 10]

$a_1^1 = 0{\cdot}2,\ b_1^1 = 0{\cdot}4,\ a_2^1 = 0{\cdot}2,\ b_2^1 = 0{\cdot}4$

$a_1^2 = 0{\cdot}6,\ b_1^2 = 0{\cdot}8,\ a_2^2 = 0{\cdot}2,\ b_2^2 = 0{\cdot}4$

$$a_1^3 = 0{\cdot}2,\ b_1^3 = 0{\cdot}4,\ a_2^3 = 0{\cdot}6,\ b_2^3 = 0{\cdot}8$$
$$a_1^4 = 0{\cdot}6,\ b_1^4 = 0{\cdot}8,\ a_2^4 = 0{\cdot}6,\ b_2^4 = 0{\cdot}8$$

For discretization of the corresponding LC-problems (12) we have chosen equidistant grids of step-sizes $h_{k+1} = h_k/2$, $0 \leqslant k \leqslant 4$, with $h_0 = 0{\cdot}5$.

In all cases the numerical results† clearly indicated the superiority of NMGEPT compared to MGEPT, thus illustrating the benefits of nested iteration. Indeed, computing a start-iterate on the finest grid by nested iteration, in all test examples it took at most three iterations until the final configuration of the elastic/plastic region was attained, while for this, using MGEPT with $u_l^0 = \psi_l$ as start-iterate, considerably more iterations had to be performed (except for higher values of C).

We have also tested various configurations of the multi-grid cycles, in particular the cases $\gamma_k = 1$, $0 \leqslant k \leqslant l$ ('V-cycle') and $\gamma_k = 2$, $0 \leqslant k \leqslant l$ ('W-cycle'), with smoothing only before as well as before and after the defect correction process.

As a measure for the performance of the schemes we have computed the residues

$$r_l = \left[\left(\sum_{x \in \Omega_l^{*,(1)}} |(\delta_l^2 u_l)(x) + 2C|^2 \right) / N_l^1 \right]^{1/2}$$

with respect to the inactive grid-points.

Table I shows the computed residues obtained by NMGEPT in case of test example I. (ii) ($C = 5{\cdot}0$, $l = 5$) for V-cycles and W-cycles with two smoothing iterations before or before and after the defect correction, ν counting the iterations on the finest grid. For computation of u_5^0 we have chosen $\nu = 1$ iteration on level $k = 0$ and $\nu = 2$ iterations on levels $1 \leqslant k \leqslant 4$ using $\varepsilon_k^1 = \varepsilon_k^2 = 1{\cdot}0\text{E}-3$, $0 \leqslant k \leqslant 4$, as termination criterion. In all cases the final distribution of active/inactive grid-points was reached after three iterations on level $l = 5$ (this explains the relatively poor convergence for $\nu \leqslant 3$ and, in particular, the deterioration of r_5 from $\nu = 1$ to $\nu = 2$ in column 3 of Table I).

It is clear that the application of multi-grid techniques remains meaningful as long as $k_{\min} < l$, while it does not make sense if the degree of plastification is so high in relation to the grid-size h_l that no inactive grid-point can be found on the next coarser grid Ω_{l-1}. Indeed, in this case MGEPT simply reduces to scheme EPT with respect to the fixed grid Ω_l.

For test example I. (ii) Table II gives the values of $k_{\min}$ for $l = 4$, 5, 6 and torsion angles (per unit length) $C = 2{\cdot}5$, $5{\cdot}0$ and $10{\cdot}0$.

Table I. Example I. (ii), $C = 5{\cdot}0$, $l = 5$

	$\gamma_k = 1$, $0 \leqslant k \leqslant 5$		$\gamma_k = 2$ $0 \leqslant k \leqslant 5$	
ν	$\kappa_1 = 2$, $\kappa_2 = 0$	$\kappa_1 = 2$, $\kappa_2 = 2$	$\kappa_1 = 2$, $\kappa_2 = 0$	$\kappa_1 = 2$, $\kappa_2 = 2$
1	0·89255E–2	0·88292E–3	0·91586E–4	0·25003E–4
2	0·35106E–2	0·45362E–3	0·96719E–4	0·21444E–4
3	0·82658E–2	0·19884E–3	0·42982E–4	0·15382E–4
4	0·13015E–3	0·47330E–4	0·52957E–5	0·41486E–5
5	0·25831E–4	0·52920E–5	0·18992E–6	0·96145E–7

†All reported results in this section have been obtained by computations being performed on the Cyber 175 of ZRZ, TU Berlin.

Table II. Example I. (ii)

k_{min} / l	$C=2{\cdot}5$	$C=5{\cdot}0$	$C=10{\cdot}0$
4	3	3	4
5	3	4	4
6	3	4	5

In Figures 1–4 we have represented the dependence of the plastification for various test examples on the applied torsion where active grid-points characterizing the discrete plastic region are marked by points.

Figures 5–11 show the plastification, the equipotential lines which correspond to the stress trajectories and the graph of the stress potential.

Note that the graph of the stress potential has a meaning in terms of Prandtl's membrane analogon and Nadai's sand-hill analogon which have been used in mechanical engineering for

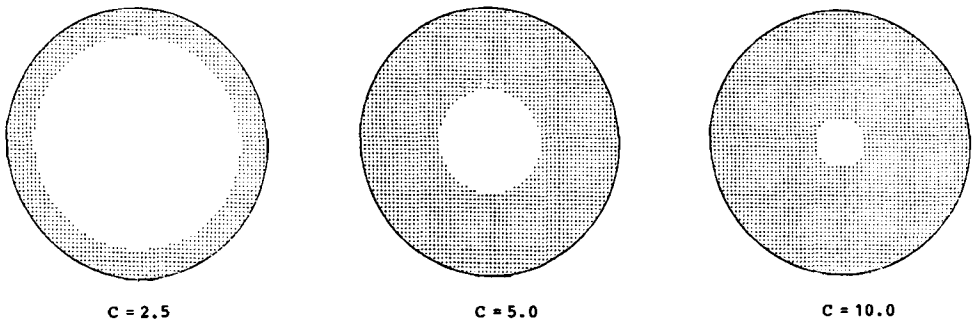

Figure 1

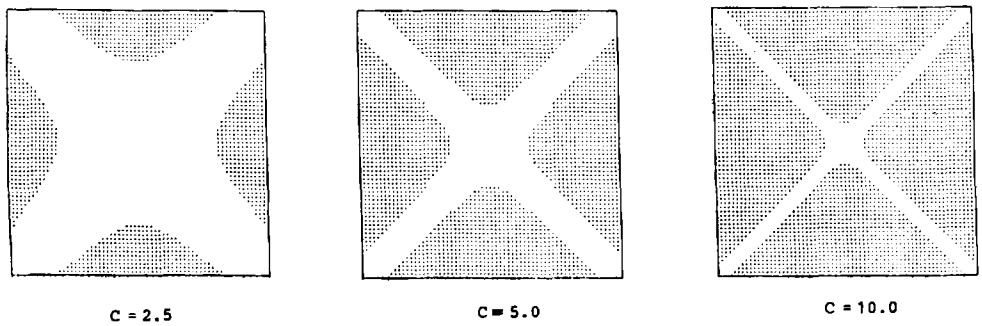

Figure 2

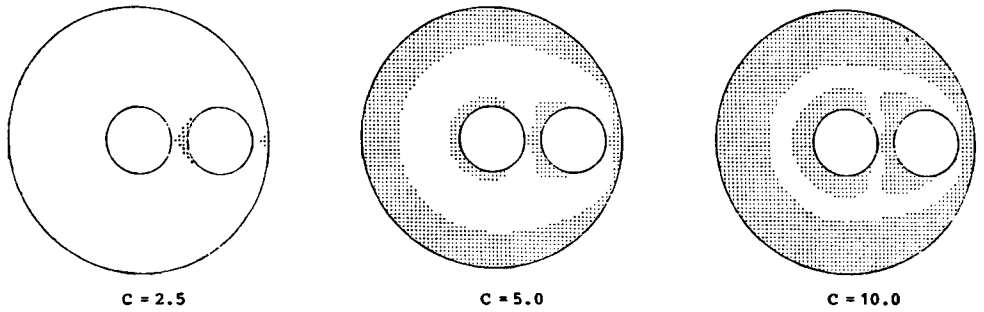

Figure 3

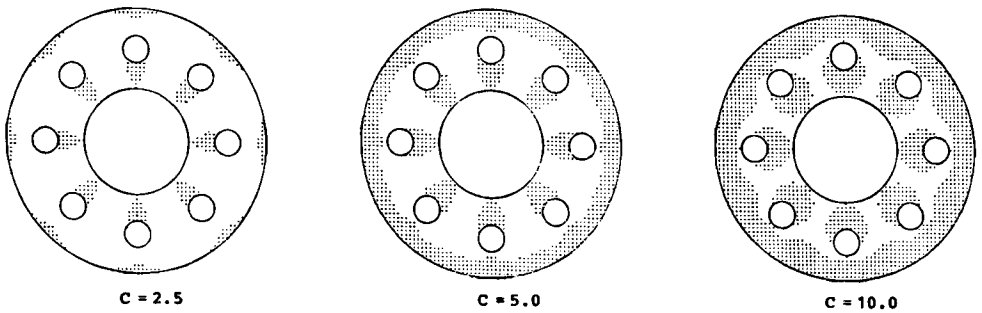

Figure 4

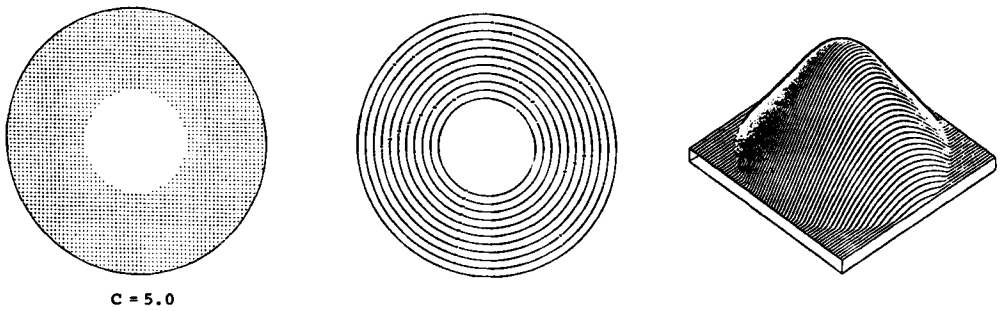

Figure 5

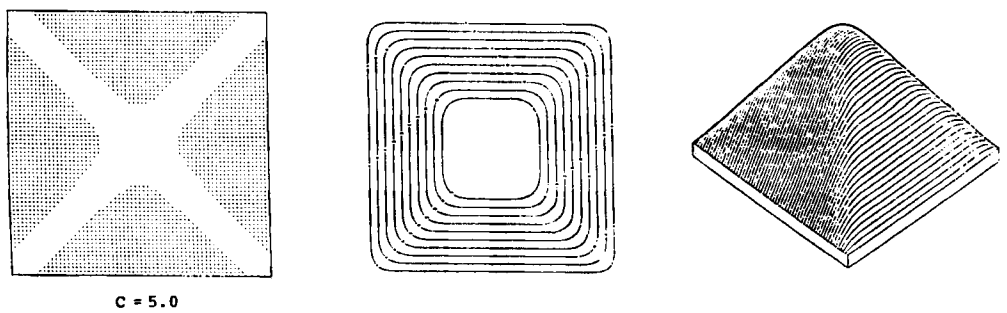

Figure 6

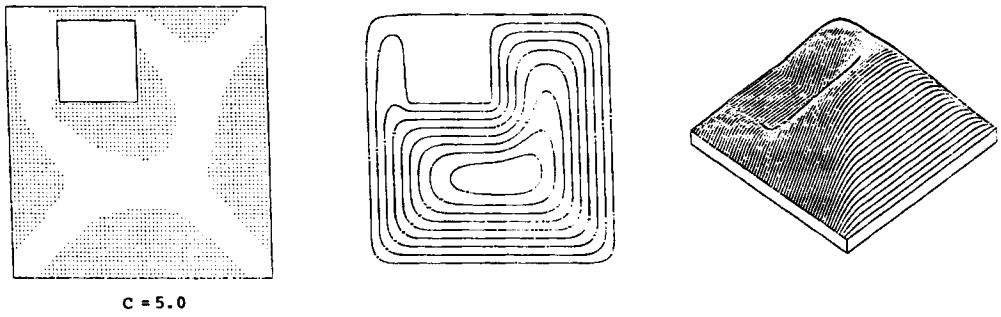

Figure 7

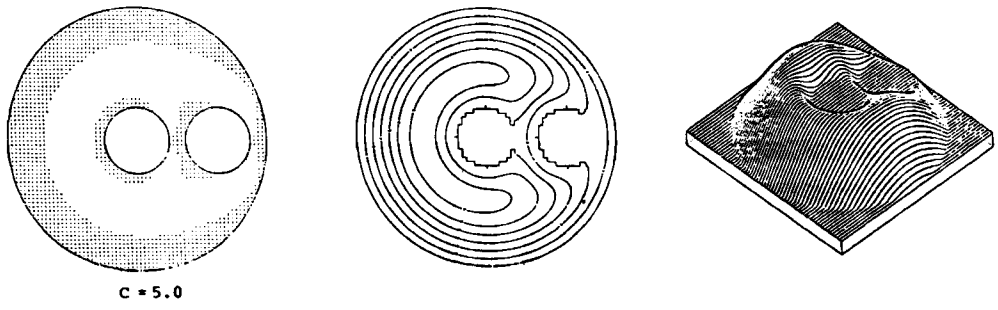

Figure 8

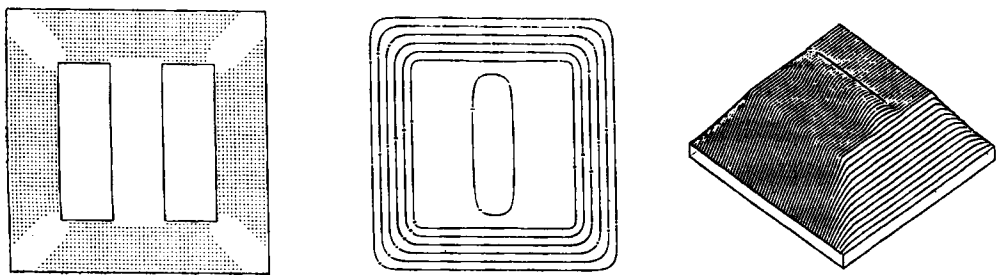

Figure 9

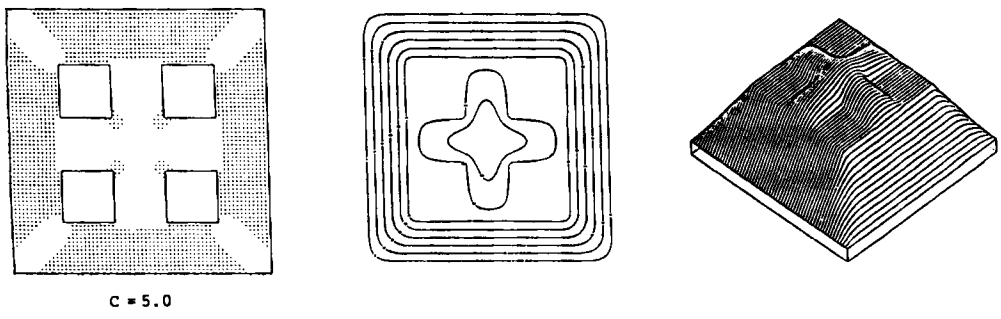

Figure 10

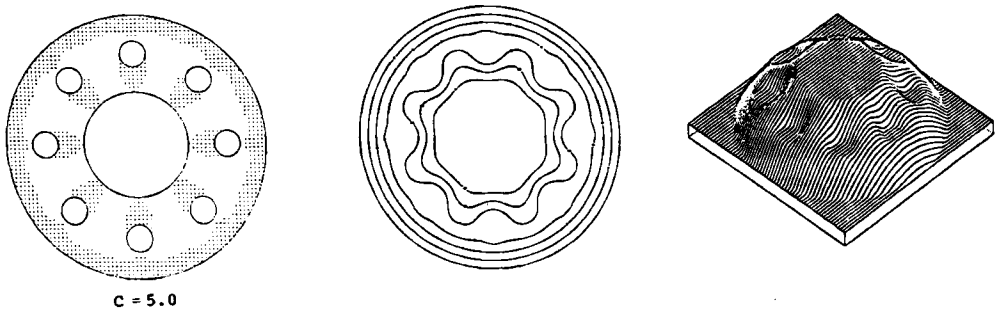

Figure 11

experimental modelling of the torsion problem. First, using transparent material a 'roof' is constructed representing the graph of the generalized distance function. Second, a membrane is put across the boundary of the cross section and finally, a pressure of magnitude $2C$ is applied to the membrane from opposite to the roof. Then, the deformation of the membrane corresponds to the stress potential, and the projection onto the plane of the boundary of the contact zones between membrane and roof indicates the free boundary between the elastic and the plastic region.

All plots shown in Figures 1–10 are based on numerical results computed on level $l = 5$ by means of the multi-grid algorithm NMGEPT.

REFERENCES

1. W. F. Ames, *Numerical Methods for Partial Differential Equations*, 2nd edn., Academic Press, New York, 1977.
2. A. Brandt and C. W. Cryer, 'Multigrid algorithms for the solution of linear complementarity problems arising from free boundary problems', *SIAM J. Sci. Stat. Comp.*, **4**, 655–684 (1983).
3. H. Brezis and M. Sibony, 'Équivalence de deux inéquations variationnelles et applications', *Arch. Rat. Mech. Anal.*, **41**, 254–265 (1971).
4. I. Ekeland and R. Temam, *Convex Analysis and Variational Problems*, North-Holland, Amsterdam, 1976.
5. R. Glowinski and H. Lanchon, 'Torsion élastoplastique d'une barre cylindrique de section multiconnexe', *J. Mech. Theor. Appl.*, **12**, 151–171 (1973).
6. R. Glowinski, J. L. Lions and R. Trémolières, *Numerical Analysis of Variational Inequalities*, North-Holland, Amsterdam, 1981.
7. W. Hackbusch, *Multi-grid Methods and Applications*, Springer, Berlin. 1985.
8. W. Hackbusch and H. D. Mittelmann, 'On multi-grid methods for variational inequalities', *Numer. Math.*, **42**, 65–76 (1983).
9. W. Hackbusch and U. Trottenberg, *Multi-grid Methods, Proceedings*, Köln-Porz, 1981, *Lecture Notes in Mathamatics.*, Vol. 960, Springer, Berlin 1982.
10. R. H. W. Hoppe, 'Multi-grid methods for Hamilton–Jacobi–Bellman equations', *Numer. Math.*, **49**, 239–254 (1986).
11. R. H. W. Hoppe, 'Multi-grid algorithms for variational inequalities', *SIAM J. Numer. Anal.* (in press).
12. H. Lanchon, 'Sur la solution du problème de torsion élastoplastique d'une barre cylindrique de section multiconnexe', *C.R. Acad. Sci. (Paris)*, Ser. I, **271**, 1137–1140 (1970).
13. P. L. Lions and B. Mercier, 'Approximation numérique des équations de Hamilton-Jacobi-Bellman', *R.A.I.R.O. Analyse Numérique/Numer. Anal.* **14**, 369–393 (1980).
14. R. Temam, *Mathematical Problems in Plasticity*, Gauthier-Villars, Paris, 1985.
15. F. Thomasset, Internal I.R.I.A. report, 1972.
16. T. W. Ting, 'Elastic plastic torsion over multiply connected domains', *Ann. Sc. Super. Pisa, Cl. Sci.*, Ser. IV, **4**, 291–312 (1977).